

Primljen / Received: 8.6.2015.
 Ispravljen / Corrected: 15.1.2016.
 Prihvaćen / Accepted: 18.3.2016.

Dostupno online / Available online: 10.6.2016.

Detection of damage to reinforced-concrete structures using piezoelectric smart aggregates

Authors:



¹ Prof. **Dragoslav Stojić**
dragoslav.stojic@gmail.com



² Prof. **Tamara Nestorović**
tamara.nestorovic@rub.de



¹ **Nemanja Marković**, MCE
nemanja.markovic@gaf.ni.ac.rs



¹ **Radovan Cvetković**, MSc. CE
radovancvetkovic@yahoo.com



³ **Nikola Stojić**, MCE
n_stojic@yahoo.com

¹University of Nis
 Faculty of Civil Engineering and Architecture

²Ruhr University Bochum
 Faculty for Civil and Environmental
 Engineering

³Highway Institute, Serbia

Original scientific paper

Dragoslav Stojić, Tamara Nestorović, Nemanja Marković, Radovan Cvetković, Nikola Stojić

Detection of damage to reinforced-concrete structures using piezoelectric smart aggregates

The implementation of active monitoring systems to diagnose damage to reinforced concrete structures using piezoelectric smart aggregates, and based on wave propagation, ranks among the world's most advanced research activities. Original models, with parametric analysis of the damage index variation problem, depending on the size, position and orientation of cracks, are presented in the paper. Numerical modelling of wave propagation in reinforced concrete is conducted using the explicit finite element method, which is highly effective for this purpose.

Key words:

piezoelectricity, structural health monitoring, finite element method, reinforced concrete

Izvorni znanstveni rad

Dragoslav Stojić, Tamara Nestorović, Nemanja Marković, Radovan Cvetković, Nikola Stojić

Otkrivanje oštećenja armiranobetonskih konstrukcija primjenom piezoelektričnih pametnih agregata

Primjena aktivnih sustava monitoringa kod otkrivanja oštećenja armiranobetonskih konstrukcija pomoću piezoelektričnih pametnih agregata, kao i na temelju širenja valova, trenutačno su najsuvremenija istraživanja u svijetu. U radu su predstavljeni originalni modeli s parametarskom analizom problema promjene indeksa oštećenja konstrukcija u ovisnosti o veličini, položaju i orijentaciji pukotina. Numeričko modeliranje širenja valova u armiranom betonu izvedeno je eksplicitnom metodom konačnih elemenata koja je veoma učinkovita za ovu uporabu.

Ključne riječi:

piezoelektričnost, monitoring konstrukcija, metoda konačnih elemenata, armirani beton

Wissenschaftlicher Originalbeitrag

Dragoslav Stojić, Tamara Nestorović, Nemanja Marković, Radovan Cvetković, Nikola Stojić

Schadensermittlung bei Stahlbetonkonstruktionen mittels intelligenter piezoelektrischer Aggregate

Die Anwendung aktiver Überwachungssysteme für die Schadensermittlung bei Stahlbetonkonstruktionen mittels intelligenter piezoelektrischer Aggregate, sowie basierend auf der Wellenausbreitung, wird derzeit in den fortschrittlichsten Untersuchungen weltweit erforscht. In dieser Arbeit werden originale Modelle einschließlich Parameteranalysen zur Veränderung des Schadensindex für Konstruktionen in Funktion der Größe, Position und Orientierung von Rissen dargestellt. Die numerische Modellierung der Wellenausbreitung im Stahlbeton wurde mittels der expliziten Finite-Elemente-Methode realisiert, die sich für diese Anwendung als sehr effizient zeigt.

Schlüsselwörter:

Piezoelektrizität, Bauwerksüberwachung, Finite-Elemente-Methode, Stahlbeton

1. Introduction

Structural Health Monitoring (SHM) is a multidisciplinary engineering area that deals with innovative methods for monitoring the safety and reliability of structures, and their integrity and characteristics, without affecting the structure or impeding its normal operation [1]. Structural Health Monitoring can be either passive or active. The paper presents an Active Structural Health Monitoring System (ASHMS) based on wave propagation and the use of piezoelectric (PZT) actuators/sensors. The ASHMS uses PZT sensors that are embedded or glued to the surface of the structure in order to monitor generation of damage, its further propagation, location, size and severity, and the effects damage can cause to the reliability and safety of structures.

In the most general terms, damage can be interpreted as a variation created in a system that exerts a negative impact on its current or future operation [2]. In this way, damage separates two states of a structure, the initial state that is often considered undamaged, and the state with the created damage. The ASHMS assisted by PZT sensors detects generation of damage if there is a reading in the two mentioned structural states – the initial undamaged state and the damaged state. Damage can occur in reinforced concrete structures for a number of reasons, which are a consequence of mechanical influences involving external load, chemical processes occurring during concrete hardening, weather and material fatigue effects, or hazardous loads such as earthquakes. The ASHMS of reinforced concrete structures must be capable of detecting damage regardless of its cause, position, size and orientation.

In recent years, the use of piezoelectric elements for active monitoring of reinforced concrete structures has been expanding and gaining an important position among the contemporary methods whose practical implementation may be expected in the future. In this context, experimental investigations of the mentioned ASHMS of RC structures with PZT SA were conducted, and their applicability for damage detection and multifunctionality was confirmed. The PZT SA were used to determine early strength of concrete in situ, and impact force in the event of vehicle collision with the RC structure, for active detection of damage, and for structural status monitoring [3, 4]. The detection and localization of errors and damage, which occur while carbon strips are glued onto reinforced-concrete beams, are presented in paper [5]. The method for detecting irregularities in the bond between reinforcement and concrete, using piezoelectric sensors inserted in the RC structure, is also presented [6]. The detection of damage to RC frame structures caused by dynamic action, in the case of bridge beams, RC walls, and piles, is experimentally analysed and presented in papers [7-10].

PZT smart aggregates can be used for new structures by building them into individual elements, fixing them to the

reinforcement or formwork at pre-designed locations, and with a defined orientation. However, these sensors can also be used for the existing buildings and, in such cases, they can be built into the slots specially designed for that purpose. Afterwards, the slots with the fitted PZT SA are filled with cement milk. Apart from placing smart aggregates into elements of the existing buildings, they can also be glued onto the element surface. Dimensions of piezoelectric elements used for that purpose ranges in most cases from 1cm to 2cm, and they can be either circular or square in form. They are fitted into a small concrete block cylindrical or cuboid in shape, depending on the form of the PZT element used. The diameter or side length of the block varies from 4cm to 8cm, and it is later fixed to the reinforcement or formwork of the element that is being built in.

Development of numerical models for PZT SA, and for propagation of waves through RC, can be of great importance for the development of the method, and for practical implementation of these models for the detection, localization and determination of damage size. Numerical models of PZT SA, and the models of wave propagation through concrete beams in damaged and undamaged condition, are presented in paper [11] using the explicit finite elements methods (EFEM). Numerical model of PZT SA for monitoring shear seismic stresses in structures using d_{15} piezoelectric mode is presented in paper [12], while the model for monitoring normal seismic stresses is developed and presented in paper [13]. The use of software package ANSYS to model PZT elements and propagation of waves through concrete beam elements for the purpose of damage detection is presented in papers [14, 15]. According to available relevant literature, some studies have been made for the purpose of developing numerical models. However, such studies are scarce, which has been a motive for writing this paper.

This paper presents very efficient numerical models that use EFEM to model propagation of waves through RC structures, as well as a parametric analysis of the damage index variation depending on crack position, crack size and crack orientation, so as to enable better understanding of the relationship between the damage index and the mentioned variable parameters.

2. Damage detection

2.1. Piezoelectric smart aggregates (PZT SA)

PZT SA have been developed for the purpose of incorporating piezoelectric elements into reinforced concrete (RC) structures. PZT SA are fitted by providing the PZT element with an appropriate waterproofing to protect it from dampness effects, by connecting it to the wiring, and by fitting it into a small concrete block. In this way, a very brittle and sensitive PZT patch is protected from dampness effects

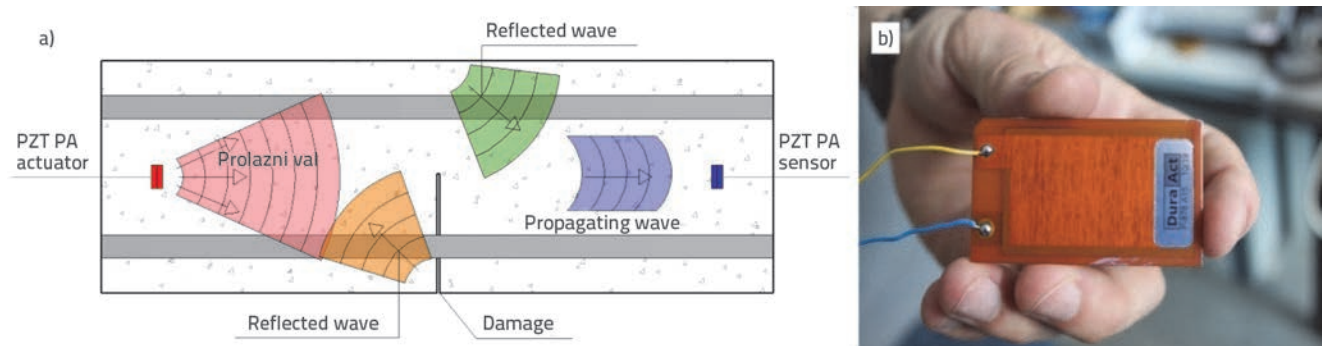


Figure 1. a) Damage detection approach; b) Piezoelectric patch DuraAct – PI Ceramics

and mechanical shocks that can occur during construction of a RC structure and during subsequent service life. The PZT SA is fitted into a RC element at an exactly determined position with a predefined orientation, which is most frequently realized by attaching it to reinforcement bars. Piezoelectric elements present a number of advantages such as: simplicity of application, low cost, fast response, high reliability, multifunctionality, resistance to chemically aggressive substances, and resistance to radioactivity and UV radiation. There are also some deficiencies: output voltage is very low requiring the use of amplifiers, high impedance, sensitivity to dampness and shocks (which is countered by making PZT SA elements waterproof and shockproof), need for a large number of PZT elements for monitoring status of a structure. Piezoelectricity is a phenomenon whereby an electric voltage is generated when a material is exposed to mechanical stress (direct effect) or, conversely, creation of mechanical deformations as a response to exposure of a material to electrical stress (counter-effect). For linear piezoelectric materials, constitutive equations of the relationship between mechanical and electric variables are presented in the matrix form [16]

$$\{S\} = [s]\{T\} + [d]^t \{E\} + \{\alpha\} \theta \quad (1)$$

$$\{E\} = [g]\{T\} + [\beta]\{D\} + \{\tilde{E}\} \theta \quad (2)$$

where:

$\{S\}, \{T\}$ - vector of mechanical strains and stresses

$\{E\}, \{D\}$ - vector of electric field and electric displacement field

θ - temperature

$\{\alpha\}, \{\tilde{E}\}$ - coefficient of thermal expansion and coefficient of piezoelectric stress

$[d]^t, [g]$ - matrices of piezoelectric stress and strain constants

$[\beta]$ - matrices of dielectric constants

$[s]$ - matrix of proportionality.

Equation (1) is also called the actuator equation and it is used to predict the magnitude of strain caused by the imparted stress, electric field and temperature. Contrary to that, equation (2) represents the equation of the sensors used to predict

electric voltage resulting from the imparted stress, electric displacement field, and temperature.

2.2. Principle of method based on wave propagation

The piezoelectric counter effect is used for actuators to enable wave propagation through a reinforced concrete element. By applying electrical voltage in an extremely short time signal (tone burst Hanning windowed signals), or continuously through time (sweep sine signals), the static condition is disturbed and the wave propagation is initiated. Contrary to that, a direct piezoelectric effect is used for sensors, i.e. to receive the incoming wave and convert the mechanical wave into electrical voltage that reads as a sensor output signal. If damage develops in a structure, it will cause variations in wave propagation through the RC element, i.e. the wave that reaches the sensor will have less energy than the reference wave from an undamaged structure (Figure 1.a). By monitoring variations of the output signal from the PZT SA sensor, it is possible to detect initiation of damage and its further propagation. Owing to its piezoelectric properties (direct and contrary piezoelectric effects), the same PZT SA can be used as both the actuator and sensor, which can considerably reduce the number of piezoelectric patches for monitoring status of a RC structure.

3. Numerical wave propagation modelling

Wave propagation modelling based on the standard finite element method is very inefficient for the numerically demanding models. In order to overcome this problem, efficient, reliable and sufficiently accurate methods must be used in numerical analysis. One of such methods is the explicit finite elements method (EFEM). The EFEM makes use of the central difference method for calculating displacements, velocities and accelerations in the form presented in equations (3) and (4):

$$\ddot{U}^{(t)} = \frac{1}{\Delta t^2} (U^{(t-\Delta t)} - 2U^{(t)} + U^{(t+\Delta t)}) \quad (3)$$

$$\dot{U}^{(t)} = \frac{1}{2\Delta t} (-U^{(t-\Delta t)} + U^{(t+\Delta t)}) \quad (4)$$

where:

Δt - time increment

U - displacement

\dot{U} - velocity

\ddot{U} - acceleration.

The solution in the time moment $tt + \Delta t$ uses the equilibrium in time t and $tt - \Delta t$, which classifies this method among explicit integration methods. This integration method does not require factorizing the rigidity matrix in each time increment, as it is the case with the implicit method, but is in fact performed only at the beginning of the calculation, which significantly reduces the simulation calculation time. Numerical efficiency of the EFEM is not only due to implementation of the explicit integration procedure, but also to the use of the diagonal mass matrix, whose inverse matrix can be determined very quickly. For the same time increment, the implicit FEM provides a more accurate solution in comparison with the explicit FEM. However, due to its high efficiency the EFEM can use a large number of small time increments and provide the desired accuracy of the solution considerably faster than the implicit method. The explicit procedure performs integration through time employing the central difference method and certain number of small time increments, which must satisfy a stable solution, i.e. the time increment employed in the model must be lower than the critical:

$$\Delta t \leq \Delta t_{crit} = \frac{2}{\omega_{max}} \tag{5}$$

$$\Delta t \leq \Delta t_{crit} = \frac{\Delta L}{c_L} \tag{6}$$

where:

ω_{max} - maximum frequency

ΔL - the least characteristic length of the finite element

c_L - wave propagation velocity.

The number of finite elements per one wavelength (n) is a very important characteristic of the model and it has a considerable effect on the accuracy of the solutions. It is recommended that n should not be lower than 7 for modelling propagation of lower frequency waves, while the values from 10 to 20 should be assumed for the very short impulse loads. When high frequency waves entering the ultrasonic range are modelled, there is a problem of a large number of finite elements in the model which, from the engineering point of view, represents very small models requiring very powerful computers with a high memory capacity. This problem can be solved by modelling the part of the model that is interesting for the analysis, which would be bordered by the absorbing layer using increasing damping (Absorbing layer using increasing damping - ALID) [17]. By using this method, the reflection of the waves from the limits of the models, which does not exist in actual large beams, is eliminated.

4. Wavelet signal analysis and formation of damage index

The output signal S of the sensor can be decomposed into 2^n signals designated as $\{X_1, X_2, \dots, X_{2^n}\}$, whereby every signal can be represented in the following manner:

$$X_j = [x_{j,1}, x_{j,2}, \dots, x_{j,m}] \tag{7}$$

where:

m - represents the number of recorded (measured) time signal data

n - represents the level of wavelet signal decomposition, $n=3$ is assumed in the paper.

Wavelet signal decomposition provides two singles called the approximation and the detail. The approximation provides information about lower signal frequencies, and the detail about higher frequencies. The energy of output signal approximations for the models presented in this paper are multiple times higher than the energy of the details. Since the damage index is based on the monitoring of the output signal energy variations, the approximations were more important in this analysis than the details. The energy of decomposed signals can be represented by the following expression:

$$E_{i,j} = \|X_j\|_2^2 = x_{j,1}^2 + x_{j,2}^2 + \dots + x_{j,m}^2 \tag{8}$$

Where: i is the time index and j is the frequency range ($j=1, 2, \dots, 2^n$). By calculating the energy of all decomposed signals, the energy vector can be calculated for an RC element in the undamaged state E_h as well as for an element in the damaged state E_o :

$$E_h = [E_{h,1}, E_{h,2}, \dots, E_{h,2^n}] \tag{9}$$

$$E_o = [E_{o,1}, E_{o,2}, \dots, E_{o,2^n}] \tag{10}$$

The damage index based on the output signal energy variation is formed as a root-mean-square-deviation:

$$DI = \sqrt{\frac{\sum_{j=1}^{2^n} (E_{o,j} - E_{h,j})^2}{\sum_{j=1}^{2^n} E_{h,j}^2}} \tag{11}$$

The damage index (DI) can have values from 0 for an undamaged structure to 1 for a totally damaged structure when the wave can not reach the sensor. Also, it can be concluded from equation (11) that the higher the difference between the output signal energy of a damaged and an undamaged RC structure, the higher the damage index. Based on this fact, it is possible to monitor the damage of a RC structure over time, by monitoring variation of the damage index.

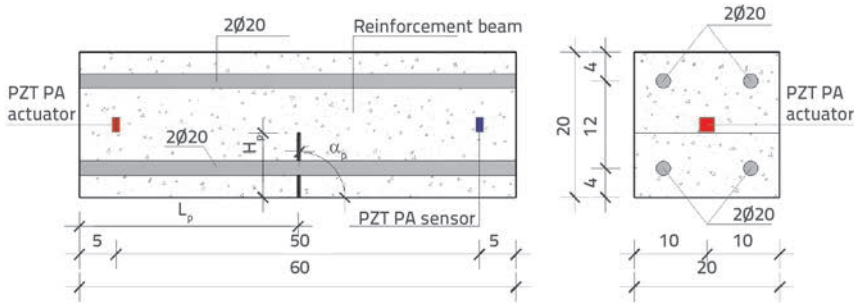


Figure 2. Geometrical characteristics of RC elements

5. Models

5.1. Geometrical characteristics

The analysed model is a reinforced-concrete element measuring 0.6x0.2x0.2 m, with the 4Ø20 reinforcement and with two PZT SA (Figure 2). A parametric analysis of the damage index variation was performed, depending on the position (L_p), size (H_p), and orientation (α_p) of the crack in the mentioned RC element. A total of 80 models were analysed, and their characteristics and designations are presented in tables 1 and 2.

The position of the crack was varied from 0.15 m to 0.45 m, with the increment of 0.05 m. The crack lengths of 0.05, 0.08, 0.11 i 0.14 m were analysed, as well as the crack angles from 60° to 120° with 10° counterclockwise increments.

Table 1. Markings and characteristics of models with vertical cracks

Parameters	Model name					Parameters	Model name				
	Model 1						Model 2				
	M 1-1	M 1-2	M 1-3	M 1-4	M 1-5	M 2-1	M 2-2	M 2-3	M 2-4	M 2-5	
L_p [m]	0.15					L_p [m]	0.20				
H_p [m]	0	0.05	0.08	0.11	0.14	H_p [m]	0	0.05	0.08	0.11	0.14
α_p [°]	90					α_p [°]	90				
	Model 3						Model 4				
	M 3-1	M 3-2	M 3-3	M 3-4	M 3-5		M 4-1	M 4-2	M 4-3	M 4-4	M 4-5
L_p [m]	0.25					L_p [m]	0.30				
H_p [m]	0	0.05	0.08	0.11	0.14	H_p [m]	0	0.05	0.08	0.11	0.14
α_p [°]	90					α_p [°]	90				
	Model 5						Model 6				
	M 5-1	M 5-2	M 5-3	M 5-4	M 5-5		M 6-1	M 6-2	M 6-3	M 6-4	M 6-5
L_p [m]	0.35					L_p [m]	0.40				
H_p [m]	0	0.05	0.08	0.11	0.14	H_p [m]	0	0.05	0.08	0.11	0.14
α_p [°]	90					α_p [°]	90				
	Model 7						Model 8 - healthy beam				
	M 7-1	M 7-2	M 7-3	M 7-4	M 7-5		M 8-1	M 8-2	M 8-3	M 8-4	M 8-5
L_p [m]	0.45					L_p [m]	0				
H_p [m]	0	0.05	0.08	0.11	0.14	H_p [m]	0				
α_p [°]	90					α_p [°]	0				

5.2. FEM modelling principle

The PZT SA on the left side of the beam was used as an actuator to perform the wave propagation, while the right side PZT SA was used as a sensor. The PZT SA model was made using the software package ABAQUS/STANDARD taking into consideration electromechanical characteristics of piezoelectric materials, and using the combination of mechanical equilibrium and the equation of equilibrium

of electrical flux. Mechanical equilibrium is presented with the equation (12):

$$\int_V \sigma : \delta \epsilon dV = \int_s t \cdot \delta u ds + \int_V f \cdot \delta u dV \quad (12)$$

where is:

σ - Cauchy stress

t - sliding of the point in the plane

f - force per volume unit,

The electrical flux equilibrium is presented with the following equation:

$$\int_V q : \delta E dV = \int_s q_s \cdot \delta \phi ds + \int_V q_v \cdot \delta \phi dV \quad (13)$$

where:

q - electrical flux

q_s - electrical flux by area unit inside a body
 q_v - electrical flux by volume unit.

Displacements obtained as a consequence of imparting electrical voltage onto the PZT element were used as an input parameter for wave propagation modelling, using the ABAQUS/EXPLICIT software package. The displacement variation function used in the analysis is the 3.5-cycle Hanning windowed tone burst signal with the duration of $3.5e^{-5}$ sec and central frequency of 100 kHz. The modelling method, employing standard and explicit FEM represents the modelling procedure used in paper [11] which was verified by an experiment involving concrete beams.

Concrete and reinforcement were modelled as linear-elastic materials, and their characteristics are presented in Table 3. The contact between the concrete and reinforcement was defined with the aid of the Tie Constraint surface contact available in ABAQUS/EXPLICIT analysis with the potential for rotational

degrees of freedom. The crack was modelled as an opening in the model, with the thickness of a finite element, and with the length and orientation defined separately for each individual model. The use of the finite-element irregular forms was required for making the grid around the slant cracks. The total duration of the simulation was $T_{sim} = 0.001$ (s), and the adopted time increment was $\Delta t = 2e^{-7}$ (s), which satisfies the critical time increment. The applied finite elements (FE) were C3D8R eight-node prismatic FE with reduced integration and Hourglass control. Twelve finite elements per one wavelength were adopted. An approximate size of the FE used in the presented models was 0.0025 m, which required around 1700000 FE for modelling the analysed RC elements.

6. Results and discussion

The wave propagation through reinforced concrete elements with and without damage is presented in figures 3-5. The

Table 2. Markings and characteristics of models with inclined cracks

Parameters	Model name					Parameters	Model name				
	Model 9						Model 10				
	M 9-1	M 9-2	M 9-3	M 9-4	M 9-5		M 10-1	M 10-2	M 10-3	M 10-4	M 10-5
L_p [m]	0.30					L_p [m]	0.30				
H_p [m]	0	0.05	0.08	0.11	0.14	H_p [m]	0	0.05	0.08	0.11	0.14
α_p [°]	120					α_p [°]	110				
	Model 11						Model 12				
	M 11-1	M 11-2	M 11-3	M 11-4	M 11-5		M 12-1	M 12-2	M 12-3	M 12-4	M 12-5
	L_p [m]	0.30					L_p [m]	0.30			
H_p [m]	0	0.05	0.08	0.11	0.14	H_p [m]	0	0.05	0.08	0.11	0.14
α_p [°]	100					α_p [°]	90				
	Model 13						Model 14				
	M 13-1	M 13-2	M 13-3	M 13-4	M 13-5		M 14-1	M 14-2	M 14-3	M 14-4	M 14-5
	L_p [m]	0.30					L_p [m]	0.30			
H_p [m]	0	0.05	0.08	0.11	0.14	H_p [m]	0	0.05	0.08	0.11	0.14
α_p [°]	80					α_p [°]	70				
	Model 15						Model 16 - healthy beam				
	M 15-1	M 15-2	M 15-3	M 15-4	M 15-5		M 16-1	M 16-2	M 16-3	M 16-4	M 16-5
	L_p [m]	0.30					L_p [m]	0			
H_p [m]	0	0.05	0.08	0.11	0.14	H_p [m]	0				
α_p [°]	60					α_p [°]	0				

Table 3. Material properties of concrete and reinforcement

Concrete			Reinforcement		
ρ [kg/m³]	E [Pa]	ν	ρ [kg/m³]	E [Pa]	ν
2400	$30 \cdot 10^9$	0.2	7800	$210 \cdot 10^9$	0.3

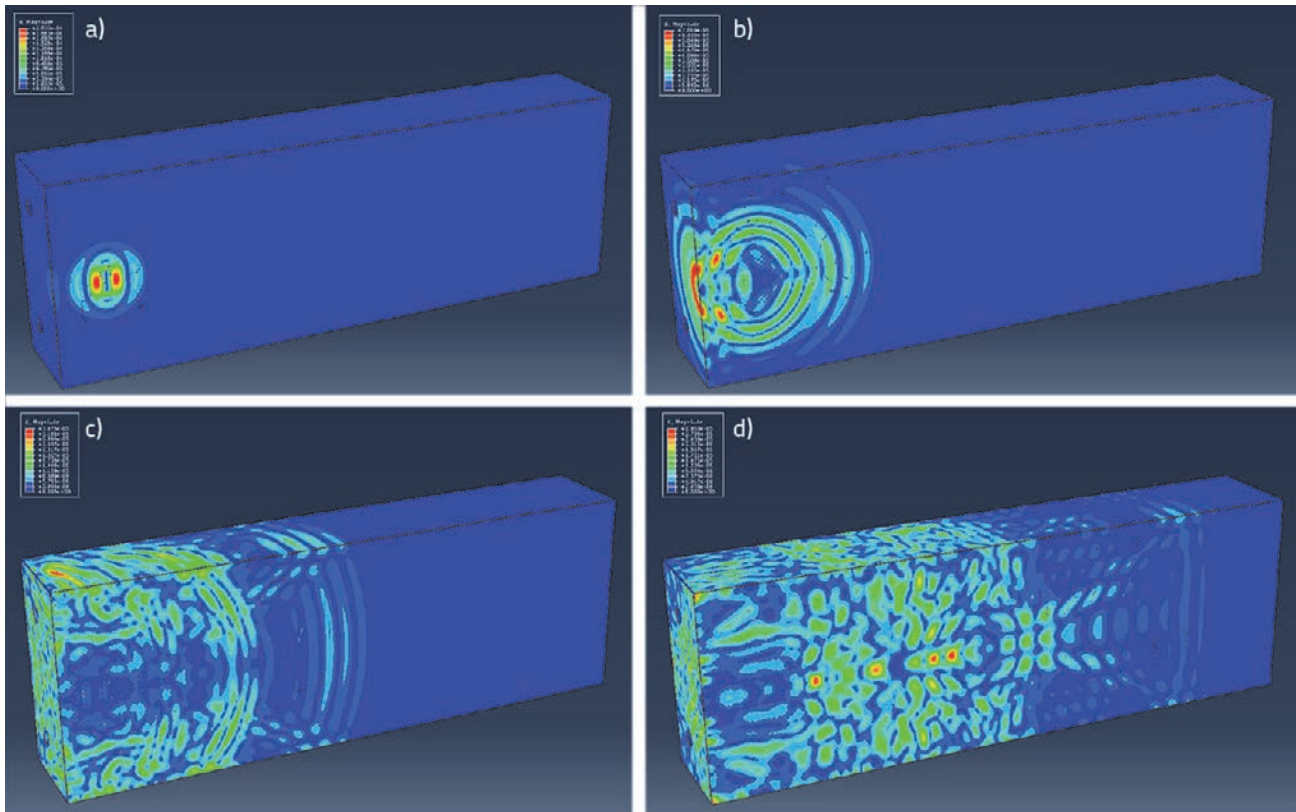


Figure 3. Wave propagation in healthy Models 8 i 16 caused by PZT PA actuator at different time intervals: a) $t=2,0172e^{-5}$ s; b) $t=4,0172e^{-5}$ s; c) $t=8,0172e^{-5}$ s; d) $t=1,4017e^{-4}$ s

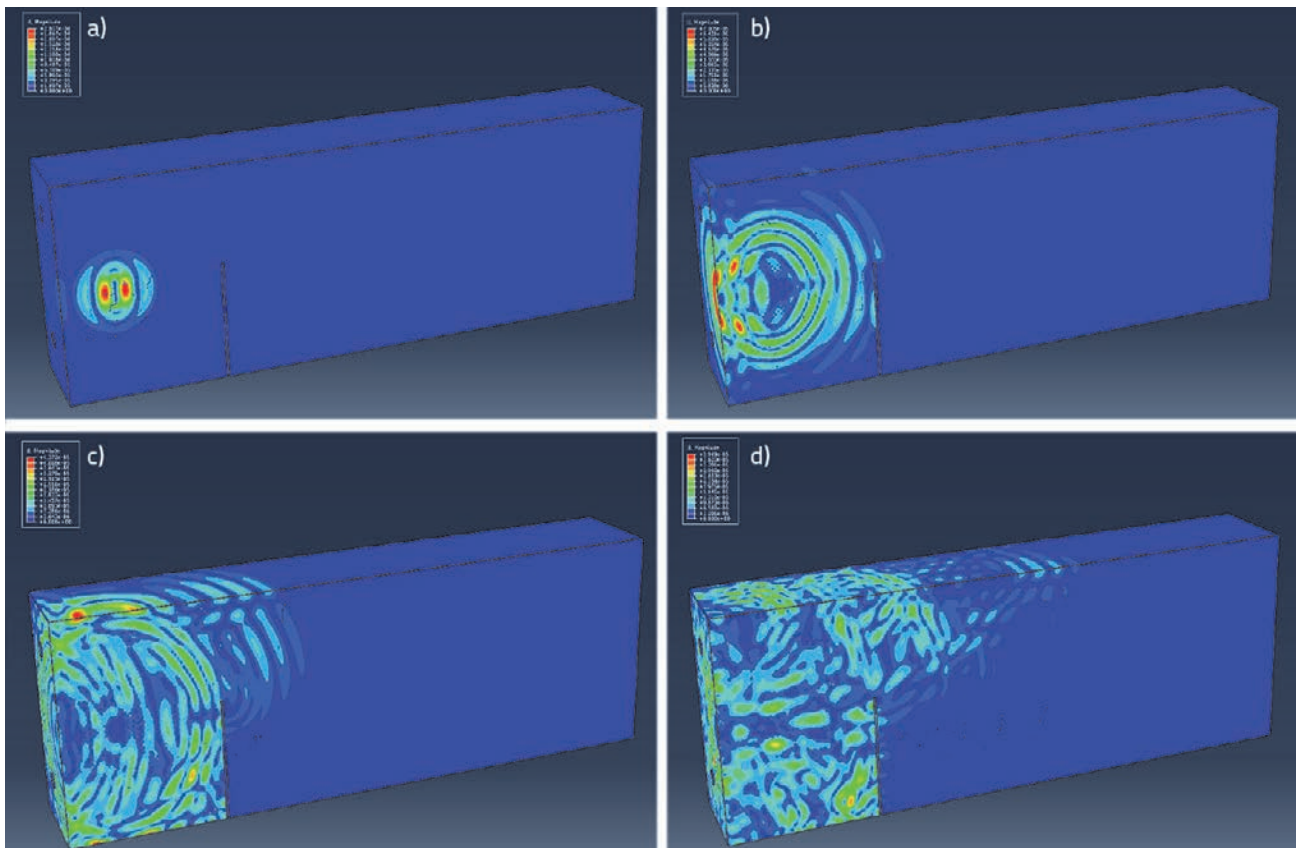


Figure 4. Wave propagation in Model 1 with vertical crack caused by PZT PA actuator at different time intervals: a) $t=2,0172e^{-5}$ s; b) $t=4,0172e^{-5}$ s; c) $t=6,0172e^{-5}$ s; d) $t=1,0017e^{-4}$ s

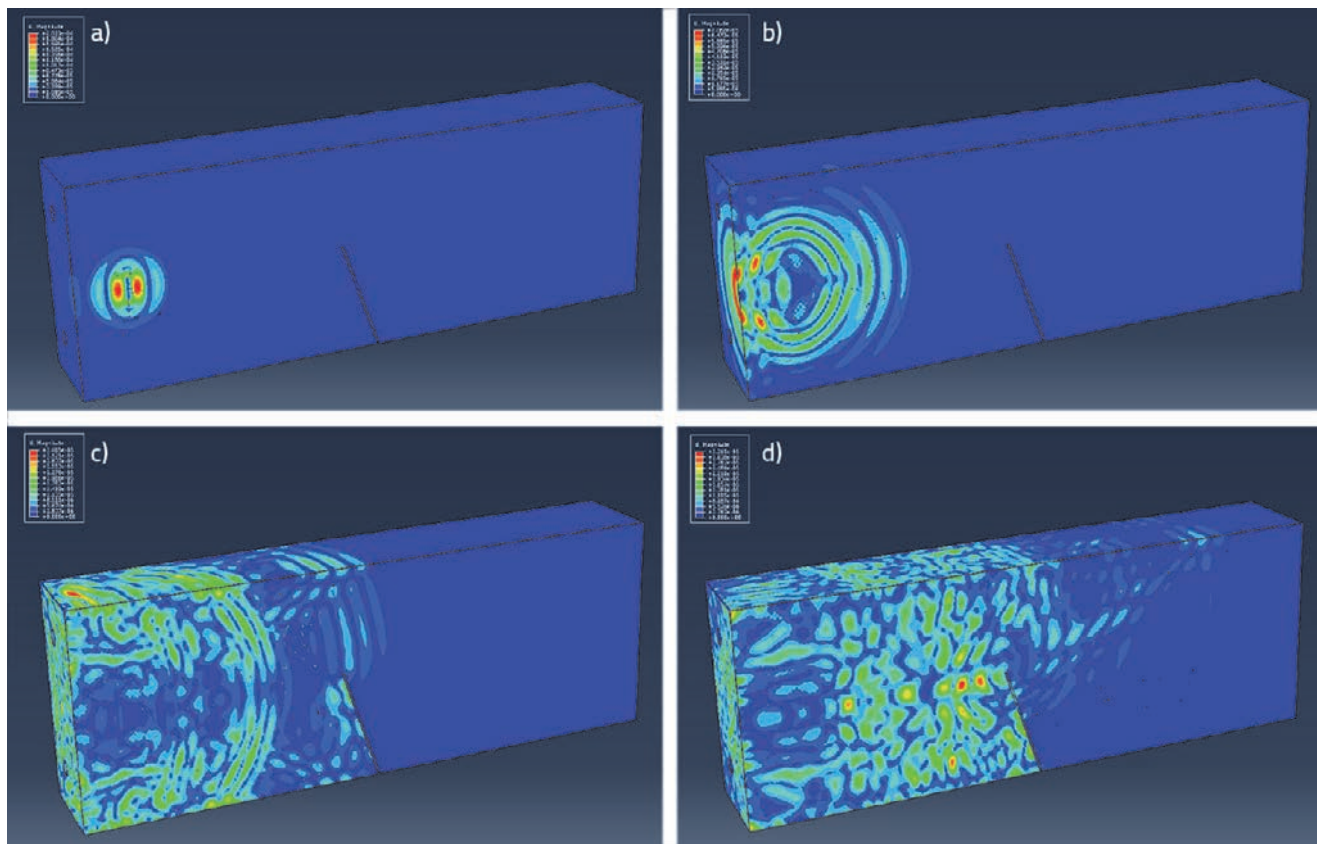


Figure 5. Wave propagation in Model 10 with inclined crack caused by PZT PA actuator at different time intervals: a) $t=2,0172e^{-5}$ s; b) $t=4,0172e^{-5}$ s; c) $t=8,0172e^{-5}$ s; d) $t=1,4011e^{-4}$ s

elements were cut through the medium vertical plane in the direction of the RC element in order to better display propagation of waves inside the reinforced concrete elements. The propagation of waves proceeds unimpeded in case of undamaged RC elements. In this case, waves travel through elements, and reflect only from external boundaries of the elements, as can clearly be seen in figures 3.a-3.d.

It can be seen in figures 4.b, 4.c, and 4.d that some of the waves reflect from the cracks and return to the actuator, weakening the propagating waves and reducing the output signal energy. Other waves pass near the cracks, propagating through the RC element and reaching the PZT SA sensor. The models with crack lengths of 0.11 and 0.14 m are characterized by the delay of the waves directly coming to the sensor, which is not the case with the models having cracks of 0.05 and 0.08 m. This can be explained by the fact that the cracks longer than 0.1 m pass through the PZT SA actuator-sensor direction. Figures 6 and 7 show damage index values for the analyzed models, depending on the crack position, length, and orientation. The values are presented on the geometry of numerical models in

order to monitor more easily the change of the damage index for the models with vertical (Figure 6) and slant cracks (Figure 7).

It can be seen in Figure 6 that change of the damage index as related to the crack position is not drastic, and that the values most frequently differ up to several percent only (Table 4). Also, the shape of the damage index variation is convex for the models with the crack length of 0.05 m, while the shape is concave in case of the models having crack lengths of 0.11 and 0.14 m. The model with the crack length of 0.08 m has approximately the same damage index values, with the mildly convex trend. Based on the results obtained in such way, it can be concluded that

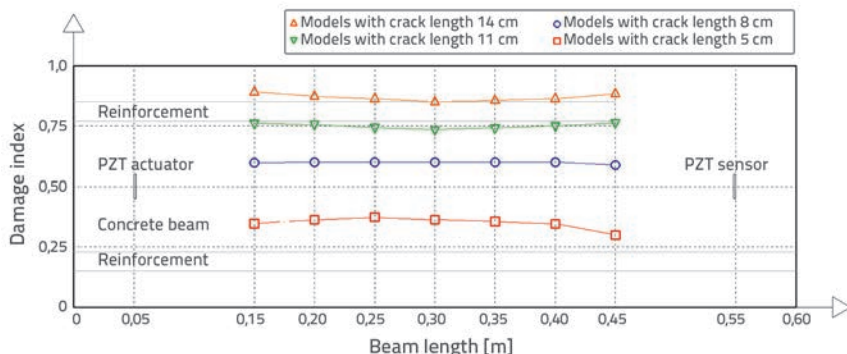


Figure 6. Damage index value depending on the position and size of vertical cracks

Table 4. Percentage deviation of DI compared to comparative model

Comparative model	Percentage deviation						Comparative model	Percentage deviation					
	$P = \left \frac{DI_i - DI_u}{DI_u} \right [\%]$							$P = \left \frac{DI_i - DI_u}{DI_u} \right [\%]$					
M 4-2	M 1-2	M 2-2	M 3-2	M 5-2	M 6-2	M 7-2	M 12-2	M 9-2	M 10-2	M 11-2	M 13-2	M 14-2	M 15-2
DI = 0.3758	4.00	0.00	2.83	2.34	5.45	16.5	DI = 0.3758	9.35	1.74	0.15	0.01	2.34	9.35
M 4-3	M 1-3	M 2-3	M 3-3	M 5-3	M 6-3	M 7-3	M 12-3	M 9-3	M 10-3	M 11-3	M 13-3	M 14-3	M 15-3
DI = 0.6046	0.32	0.00	0.28	0.22	0.00	2.13	DI = 0.6046	3.29	4.97	0.17	0.14	4.98	3.30
M 4-4	M 1-4	M 2-4	M 3-4	M 5-4	M 6-4	M 7-4	M 12-4	M 9-4	M 10-4	M 11-4	M 13-4	M 14-4	M 15-4
DI = 0.7347	3.41	2.72	1.03	0.95	2.09	3.83	DI = 0.7347	0.08	2.44	3.09	3.07	2.44	0.12
M 4-5	M 1-5	M 2-5	M 3-5	M 5-5	M 6-5	M 7-5	M 12-5	M 9-5	M 10-5	M 11-5	M 13-5	M 14-5	M 15-5
DI = 0.8498	4.74	2.64	1.51	0.73	1.69	4.13	DI = 0.8498	2.95	1.45	1.52	1.49	1.47	2.84

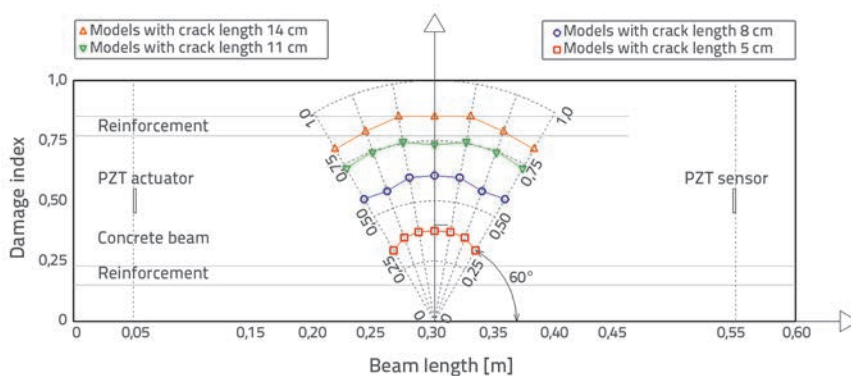


Figure 7. Damage index value depending on the orientation and size of inclined cracks

the DI variation is approximately convex if the crack is smaller than the PZT SA actuator-sensor direction, while the variation is approximately concave for the crack values larger than this position. The observed phenomenon is in the direct relation with the position of the PZT SA actuator and sensor, geometry of RC element, position of reinforcement in the beam, and the position and size of the damage. Due to all these parameters affecting variation of DI, it is not possible to provide a rule of the damage index variation function depending on the position, length, and orientation of the crack.

In case of the model with slant cracks (Figure 7), the variation of damage index depending on the gradient of the cracks does not exceed 5% except in the case of the models M 9-2 and M 15-2. Also, the models with vertical cracks do not exceed the mentioned percentage except for the models M 7-2 and M 6-2. A small percentage of DI variation depending on the position and orientation of the crack leads to the conclusion that DI is

in direct relation to the size of the crack, position of the PZT SA actuator-sensor, and the RC beam geometry, and that it does not greatly depend on the position and orientation of the damage.

The presented damage detection based on wave propagation and PZT SA does not provide potential for determining position of the damage, and its size and orientation. Thus, further work is needed in order to develop the methods which will provide an answer to these questions and improve the existing method.

7. Conclusion

The procedure for active monitoring of the status of RC structures, and for detection of damage based on wave propagation, using piezoelectric smart aggregates placed within the structure, is presented in the paper. Smart aggregates are very up-to-date multifunctional devices characterized by low cost, very fast response, wide frequency range, simple use, and high resistance to weather effects, radioactivity, UV radiation and chemically aggressive substances. Damage development is monitored using a one-dimensional damage index based on the "wavelet" signal analysis. The paper presents original numerical models depicting wave propagation through RC beams with or without damage, using the explicit finite element method characterized by an excellent efficiency. Also, a parametric analysis of the damage index variation was performed, in relation to the length, position and orientation of cracks in RC beams. On the basis of the obtained

results, it can be concluded that the change of the damage index in relation to the position and orientation of the crack does not exceed several percent in most models. The damage index value can range between 0, in case of an undamaged structure, to 1, in case of a completely damaged structure, and is mostly dependent on the size of the damage, regardless of its position or its orientation.

The damage index directly depends on the position of the PZT SA sensor-actuator, size, frequency and location of damage, geometry of RC beam, and position of the reinforcement. A certain dependence of the damage index variation on the position of the crack and its gradient was observed on the basis of the parametric analysis conducted in this paper.

REFERENCES

- [1] Stepinski, T., Uhl, T., Staszewski, W.: *Advanced structural damage detection - From theory to engineering applications*, John Wiley and Sons, West Sussex, United Kingdom, pp. 1-17, 2013., <http://dx.doi.org/10.1002/9781118536148>
- [2] Deraemaeker, A., Worden, K.: *New trends in vibration based structural health monitoring*, Springer-Verlag, Wien and New York, pp. 1-19, 2010.
- [3] Song, G., Gu, H., Mo, Y.L.: *Smart aggregates: multi-functional sensors for concrete structures - a tutorial and a review*, *Smart Materials and Structures*, 17 (2008) 3, pp. 1-17, <http://dx.doi.org/10.1088/0964-1726/17/3/033001>
- [4] Song, G., Olmi, C., Gu, H.: *An overheight vehicle - bridge collision monitoring system using piezoelectric transducers*, *Smart Material and Structures*, 16 (2007) 2, pp. 462-468, <http://dx.doi.org/10.1088/0964-1726/16/2/026>
- [5] Kim, J.W., Lee, C., Park, S.: *Damage localization for CFRP-debonding defects using piezoelectric SHM techniques*, *Research in Nondestructive Evaluation*, 23 (2012), pp. 183-196, <http://dx.doi.org/10.1080/09349847.2012.660244>
- [6] Wu, F., Chang, F.K.: *Debond Detection using Embedded Piezoelectric Elements for Reinforced Concrete Structures - Part II: Analysis and Algorithm*, *Structural Health Monitoring*, 17 (2006), pp. 17-28, <http://dx.doi.org/10.1177/1475921706057979>
- [7] Laskar, A., Gu, H., Mo, Y.L., Song, G.: *Progressive collapse of a two-story reinforced concrete frame with embedded smart aggregates*, *Smart Materials and Structures*, 18 (2009) 7, pp. 10, <http://dx.doi.org/10.1088/0964-1726/18/7/075001>
- [8] Song, G., Gu, H., Mo, Y.L., Hsu, T.T.C., Dhonde, H.: *Concrete structural health monitoring using embedded piezoceramic transducers*, *Smart Materials and Structures*, 16 (2007) 4, pp. 959-968, <http://dx.doi.org/10.1088/0964-1726/16/4/003>
- [9] Yan, S., Sun, W., Song, G., Gu, H., Huo, L.S., Liu, B., Zhang, Y.G.: *Health monitoring of reinforced concrete shear walls using smart aggregates*, *Smart Materials and Structures*, vol. 18, 2009.
- [10] Wang, R.L., Gu, H., Mo, Y.L., Song, G.: *Proof-of-concept experimental study of damage detection of concrete piles using embedded piezoceramic transducers*, *Smart Materials and Structures*, vol. 22, 2013.
- [11] Markovic, N., Nestorovic, T., Stojic, D.: Numerical modeling of damage detection in concrete beams using piezoelectric patches, *Mechanics Research Communications*, 64 (2015), pp. 15-22, <http://dx.doi.org/10.1016/j.mechrescom.2014.12.007>
- [12] Hou, S., Zhang, H.B., Ou, J.P.: A PZT-based smart aggregate for seismic shear stress monitoring, *Smart Materials and Structures*, 22 (2013) 6, pp. 9, <http://dx.doi.org/10.1088/0964-1726/22/6/065012>
- [13] Hou, S., Zhang, H.B., Ou, J.P.: A PZT-based smart aggregate for compressive seismic stress monitoring, *Smart Materials and Structures*, 21 (2012) 10, 9pp., doi: <http://dx.doi.org/10.1088/0964-1726/21/10/105035>
- [14] Song, F., Huanf, G.L., Kim, J.H., Haran, S.: On the study of surface wave propagation in concrete structures using a piezoelectric actuators/sensors system, *Smart Materials and Structures*, 17 (2008) 5, pp. 8, <http://dx.doi.org/10.1088/0964-1726/17/5/055024>
- [15] Park, S., Ahmad, S., Yun, C.B., Roh, Y.: Multiple Crack Detection of Concrete Structures Using Impedance-based Structural Health Monitoring Techniques, *Experimental Mechanics*, 46 (2006), pp. 609-618, <http://dx.doi.org/10.1007/s11340-006-8734-0>
- [16] Giurgiutiu, V.: *Structural health monitoring with piezoelectric wafer active sensors*, Elsevier, pp. 13-39, 2008.
- [17] Drozd, M.B.: *Efficient finite element modelling of ultrasonic waves in elastic media*, PhD thesis, Imperial college of science technology and medicine, London, 2008.